

Quantitative Proteomic and Phosphoproteomic Analysis of H37Ra and H37Rv Strains of *Mycobacterium tuberculosis*

Renu Verma,^{†,‡} Sneha Maria Pinto,[§] Arun Hanumana Patil,^{†,‡} Jayshree Advani,^{†,⊥} Pratigya Subba,[§] Manish Kumar,^{†,⊥} Jyoti Sharma,[†] Gourav Dey,^{†,⊥} Raju Ravikumar,[¶] Shashidhar Buggi,^{□,∇} Parthasarathy Satishchandra,[#] Kusum Sharma,[○] Mrutyunjay Suar,[‡] Srikanth Prasad Tripathy,[◆] Devendra Singh Chauhan,[■] Harsha Gowda,^{†,§} Akhilesh Pandey,^{†,▲,●,+} Sheetal Gandotra,^{*,□} and Thottethodi Subrahmanya Keshava Prasad^{*,†,§,||} 

[†]Institute of Bioinformatics, International Technology Park, Bangalore 560066, India

[‡]School of Biotechnology, KIIT University, Bhubaneswar, Odisha 751024, India

[§]YU-IOB Center for Systems Biology and Molecular Medicine, Yenepoya University, Mangalore 575020, India

[⊥]Manipal University, Madhav Nagar, Manipal 576104, India

[¶]Department of Neuromicrobiology, [#]Department of Neurology, and ^{||}NIMHANS-IOB Proteomics and Bioinformatics Laboratory, Neurobiology Research Centre, National Institute of Mental Health and Neurosciences, Bangalore 560029, India

[□]Intermediate Reference Laboratory, State Tuberculosis Training and Demonstration Centre, Someshwaranagar, SDSTRC and RGICD Campus, Bangalore 560029, India

[∇]Department of Cardio Thoracic Surgery, Super Specialty State Referral Hospital for Chest Diseases, Someshwaranagar First Main Road, Dharmaram College Post, Bangalore 560029, India

[○]Department of Medical Microbiology, Postgraduate Institute of Medical Education & Research (PGIMER), Chandigarh 160012, India

[◆]National Institute for Research in Tuberculosis (Indian Council of Medical Research), Chennai 600031, India

[■]Department of Microbiology, National JALMA Institute for Leprosy & Other Mycobacterial Diseases (Indian Council of Medical Research), Agra 282004, India

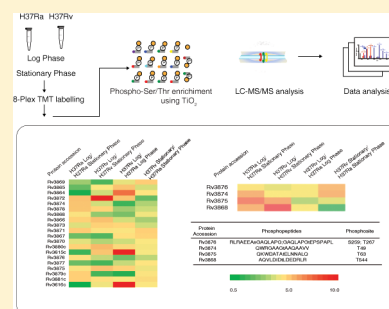
[▲]McKusick-Nathans Institute of Genetic Medicine, [●]Department of Biological Chemistry, and ⁺Department of Pathology and Oncology, Johns Hopkins University School of Medicine, Baltimore, Maryland 21205, United States

[□]CSIR-Institute of Genomics & Integrative Biology, SukhdevVihar, New Delhi 110020, India

Supporting Information

ABSTRACT: *Mycobacterium tuberculosis*, the causative agent of tuberculosis, accounts for 1.5 million human deaths annually worldwide. Despite efforts to eradicate tuberculosis, it still remains a deadly disease. The two best characterized strains of *M. tuberculosis*, virulent H37Rv and avirulent H37Ra, provide a unique platform to investigate biochemical and signaling pathways associated with pathogenicity. To delineate the biomolecular dynamics that may account for pathogenicity and attenuation of virulence in *M. tuberculosis*, we compared the proteome and phosphoproteome profiles of H37Rv and H37Ra strains. Quantitative phosphoproteomic analysis was performed using high-resolution Fourier transform mass spectrometry. Analysis of exponential and stationary phases of these strains resulted in identification and quantitation of 2709 proteins along with 512 phosphorylation sites derived from 257 proteins. In addition to confirming the presence of previously described *M. tuberculosis* phosphorylated proteins, we identified 265 novel phosphorylation sites. Quantitative proteomic analysis revealed more than five-fold upregulation of proteins belonging to virulence associated type VII bacterial secretion system in H37Rv when compared to those in H37Ra. We also identified 84 proteins, which exhibited changes in phosphorylation levels between the virulent and avirulent strains. Bioinformatics analysis of the proteins altered in their level of expression or phosphorylation revealed enrichment of pathways involved in fatty acid biosynthesis and two-component regulatory system. Our data provides a resource for further exploration of functional differences at molecular level between H37Rv and H37Ra, which will ultimately explain the molecular underpinnings that determine virulence in tuberculosis.

KEYWORDS: *chaperones, kinome, Orbitrap Fusion Tribrid mass spectrometer, proteases, proteasomes, protein abundance*



Received: November 15, 2016

Published: February 28, 2017

■ INTRODUCTION

Mycobacterium tuberculosis, the causative agent of tuberculosis (TB) has evolved successful mechanisms to overcome the host defense system and survive against existing classes of antibiotics. According to the global TB control report by the World Health Organization, an estimated 9 million people developed TB and 1.5 million died from the disease during 2014. *M. tuberculosis* H37Rv and H37Ra strains have been used in several investigations to understand the molecular mechanisms of virulence and pathogenicity.^{1–3} Comparative genomic studies have revealed 53 insertions and 21 deletions in H37Ra genome with respect to that of H37Rv. These differences could potentially cause its virulence attenuation.³ In addition, 76 SNVs affecting promoters of 32 genes were found to be specific to H37Ra. Variations have also been observed in the repetitive sequences in PE/PPE/PE–PGRS family genes in H37Ra and H37Rv. These genes have been reported to play an important role in evasion of host immune response via antigenic variation.⁴ However, elucidation of large-scale differences at the level of functional proteome between the two strains using high-resolution mass spectrometry platform remains largely unexplored.

In addition to the changes in the expression of proteins, it has been shown that variation in protein phosphorylation also plays a vital role in regulating stress adaptation, adhesion to host, virulence, and response to host immune system.^{5–7} The *M. tuberculosis* genome encodes for 11 serine/threonine protein kinases (STPKs) and 11 two-component systems. Priscic et al., have previously reported changes in phosphorylation patterns in H37Rv under different culture conditions suggesting a vital role of phosphorylation in the regulation of key physiological processes.⁸ Additionally, analysis of tyrosine phosphoproteome in H37Rv by Kusebauch et al., revealed extensive tyrosine phosphorylation on several *M. tuberculosis* proteins including STPKs.⁹ Phosphoproteomic analysis of *M. tuberculosis* Beijing isolate,¹⁰ *M. smegmatis*, and *M. bovis*¹¹ have also been carried out to demonstrate the different phosphorylation patterns in pathogenic and nonpathogenic strains. However, there has been no effort to study quantitative changes in phosphorylation levels of proteins between virulent (H37Rv) and avirulent (H37Ra) strains of *M. tuberculosis*. Alterations in the protein expression and phosphorylation patterns between the two strains can serve as the basis to gain insight into the mechanism of virulence attenuation in H37Ra strain.

In this study, we aimed at elucidating the differential expression patterns in the proteome and phosphoproteome of H37Ra and H37Rv using tandem mass tag (TMT) labeling approach coupled with high-resolution mass spectrometry. We identified several proteins that are known to be involved in the virulence and pathogenesis of *M. tuberculosis*. In addition to confirming the presence of previously described *M. tuberculosis* phosphorylated proteins, we also identified 265 sites of phosphorylation that have not been reported so far. Our data provide a resource to further explore the molecular changes on the growth and virulence of *M. tuberculosis*, which may aid in the identification of new biomarkers and therapeutic targets.

■ EXPERIMENTAL PROCEDURES

M. tuberculosis Culture and Protein Extraction

M. tuberculosis H37Rv and H37Ra were grown in Middlebrook 7H9 culture medium (BD) supplemented with OADC (oleic acid, dextrose, and catalase). Cultures were incubated at 37 °C in a roller bottle shaker. The two strains were harvested at logarithmic

($A_{600\text{ nm}} = 0.8$) and stationary phases (15 days after log phase, $A_{600\text{ nm}} \approx 5$) and centrifuged for proteomic and phosphoproteomic analysis. The cell pellets were washed thrice with chilled phosphate buffered saline. Lysis was performed in 4% SDS in Tris-HCl, pH 8.0 at 95 °C. Samples were incubated at 95 °C for 20 min followed by water bath sonication for 60 min. Lysates were resuspended in twice the volume of buffer with phosphate inhibitors (4% SDS in 50 mM triethylammonium bicarbonate (TEABC), 1 mM sodium fluoride, 1 mM sodium orthovanadate, 2.5 mM sodium pyrophosphate, 1 mM beta glycerophosphate). Protein concentration was determined using bicinchoninic acid assay (Pierce, Waltham, MA).

Trypsin Digestion and Fractionation

Equal amounts of lysate (1 mg) from each condition were processed using modified filter aided sample preparation (FASP) protocol as described earlier.¹² Briefly, the cell lysates were reduced and alkylated using 5 mM dithiothreitol (DTT) and 20 mM iodoacetamide, respectively. The SDS concentration was reduced to <0.001% using 8 M urea. Prior to trypsin digestion, the samples were buffer exchanged with 50 mM TEABC to remove urea. The samples were then incubated with trypsin (1:20) (Worthington Biochemical Corp.), and digested overnight at 37 °C. The extracted peptides were vacuum-dried and stored at –80 °C until further analysis.

TMT Labeling

Equal amounts of peptides from each condition were used for 8-plex TMT labeling (Thermo Scientific). Prior to labeling, the peptides from each condition were reconstituted in 50 mM TEABC (pH 8.0) and split into two parts to serve as technical replicates. TMT labeling was carried out as follows: H37Ra log phase replicates were labeled with channels 126 and 127N, H37Ra stationary phase-replicates with 127C and 128N, and H37Rv log phase replicates and H37Rv stationary phase replicates with 128C, 129N, 129C, and 130C, respectively. The labeling was carried out as per manufacturer's protocol. The reaction was quenched by adding 8 μL of 5% hydroxylamine and incubated at room temperature for 15 min and dried.¹³

Basic pH RPLC (bRPLC) and TiO₂-Based Phosphopeptide Enrichment

TMT-labeled peptides were fractionated using high pH reverse phase LC as described earlier.¹⁴ Briefly, the labeled peptides were resuspended in 1 mL of bRPLC solvent (10 mM TEABC pH 8.4) and fractionated using high pH reverse phase XBridge C18 column (5 μm , 250 \times 4.6 mm²) (Waters Corporation, Milford, MA) by employing an increasing gradient of bRPLC solvent B (10 mM TEABC in 90% ACN, pH 8.4). The fractionation was carried out using Agilent 1100 LC system with a flow rate of 1 mL/min. A total of 96 fractions were collected in 96-well plate containing 0.1% formic acid. The fractions were then concatenated to 12 fractions and vacuum-dried. One-tenth volume from each fraction was transferred to microcentrifuge tubes and evaporated to dryness for total proteome analysis. The remaining 90% volume from each fraction was dried and then subjected to TiO₂-based phosphopeptide enrichment.¹² The enriched phosphopeptides were eluted thrice with 40 μL of 2% ammonia solution into microfuge tubes containing 10 μL of 20% TFA on ice. The peptides were dried and resuspended in 30 μL of 0.1% TFA and desalted using C₁₈ Stage tips. The eluted peptides were subjected to LC–MS/MS analysis.

LC–MS/MS Analysis

The fractions for phosphoproteomic and total proteomic analyses were analyzed on Orbitrap Fusion Tribrid mass spectrometer (Thermo Fisher Scientific, Bremen, Germany) interfaced with Easy-nLC II nanoflow liquid chromatography system (Thermo Scientific, Odense, Denmark). The peptide digests were reconstituted in 0.1% formic acid and loaded onto trap column (75 $\mu\text{m} \times 2\text{ cm}$) packed in-house with Magic C₁₈ AQ (Michrom Bioresources, Inc., Auburn, CA, USA). Peptides were resolved on an analytical column (75 $\mu\text{m} \times 20\text{ cm}$) at a flow rate of 300 nL/min using a linear gradient of 5–40% solvent B (0.1% formic acid in 95% acetonitrile) over 90 min and total run time of 120 min. Data-dependent acquisition with full scans in 350–1500 m/z range was carried out using an Orbitrap mass analyzer at a mass resolution of 120000 at 200 m/z . Most intense precursor ions were selected at top speed data dependent mode with maximum cycle time of 3 s. Peptides with charge 2–5 were selected, and dynamic exclusion was set to 45 min. Precursor ions were fragmented using higher-energy collision dissociation (HCD) set to 34%, and MS/MS ions were detected using Orbitrap at a mass resolution of 30000 at 200 m/z . Internal calibration was carried out using lock mass option (m/z 445.120025) from ambient air.

Database Searches for Peptide and Protein Identification

Raw data files were processed to generate peak list files using Proteome Discoverer software version 2.0.1 (Thermo Fisher Scientific, Bremen, and Germany). The protein databases used for MS/MS search for H37Rv and H37Ra were downloaded from Tuberculist (Release 27- March 2013) and NCBI (updated December 12, 2012), containing 4031 and 4034 protein sequences, respectively. Reciprocal protein BLAST was carried out using *M. tuberculosis* H37Rv protein database updated with H37Ra proteins containing one or more mismatches with H37Rv proteins. Tryptic peptides were generated from these proteins *in silico* and were mapped to H37Rv protein database. Only unique tryptic peptides from H37Ra proteins were included in the database. A combined database consisting of H37Ra unique tryptic peptides, proteins from Tuberculist, and common contaminants was created (containing 6466 entries with common contaminants).

MS/MS spectra were searched against the combined protein database using SEQUEST and Mascot search algorithms through Proteome Discoverer software suite. The search parameters included trypsin as the proteolytic enzyme with one missed cleavage allowed. Oxidation of methionine was set as dynamic modification, whereas carbamidomethylation of cysteine and TMT modification at peptide N-terminus and lysine were set as static modifications. For phosphoproteomic data, phosphorylation of serine, threonine, and tyrosine was considered as additional dynamic modification. Precursor ion mass tolerance and fragment ion mass tolerance were allowed with 10 ppm and 0.05 Da, respectively, and all the PSMs were identified with 1% FDR. Reporter ions quantifier node of Proteome Discoverer was used for relative quantitation of proteins. The total proteomic and phosphoproteomic data were median-normalized. The probability of phosphorylation at each residue was calculated using PhosphoRS3.1 node in Proteome Discoverer. Phosphopeptides with >75% localization probability were considered for further analysis. Proteins and phosphopeptides with ratios greater than 2-fold were considered as regulated and used for further bioinformatics analysis.

The mass spectrometry proteomics data were deposited to the ProteomeXchange Consortium (<http://proteomecentral.proteomexchange.org>) via the PRIDE partner repository with the data set identifier PXD004161.

Bioinformatics Analysis

The differentially expressed or phosphorylated proteins identified in our study were considered for Gene Ontology analysis. The proteins were categorized according to their molecular function, biological process, and cellular components using Tuberculist–*M. tuberculosis* H37Rv database.

The total and differentially phosphorylated sites were considered for motif analysis using Motif-X algorithm.¹⁵ The parameters used have been described elsewhere,¹² and a significance threshold level was set to 0.001. The substrates and phosphorylated sites of 11 known Ser/Thr kinases of *M. tuberculosis* were curated from the literature. Thereafter, the phosphorylation levels of identified phosphosites and their motifs were overlaid with the known kinases of *M. tuberculosis* using in-house Python script.

Network Analysis of Differentially Expressed and Phosphorylated Proteins

We performed network analysis using DAVID Bioinformatics Resources 6.7.¹⁶ Proteins that showed 2-fold or more differential expression or phosphorylation at log and stationary phases between the two strains were considered for this analysis. Pathway analysis was performed to group the proteins into different functional categories and enrich particular biological pathways that may serve as the determinants for virulence in *M. tuberculosis*.

RESULTS AND DISCUSSION

Proteomic and Phosphoproteomic Profiles of Virulent and Avirulent Strains of *M. tuberculosis*

To identify phosphoproteins and signaling networks of *M. tuberculosis* that may be potentially associated with its virulence and pathogenesis, we compared the proteome and phosphoproteome of H37Rv with its avirulent counterpart H37Ra using 8-plex TMT-labeling-based quantitative proteomic approach. The proteomic and phosphoproteomic profiles of both the strains, harvested at their logarithmic and stationary phases in two technical replicates, were analyzed using LC–MS/MS. TiO₂-based enrichment strategy was followed to enrich the phosphopeptides. The combined workflow for proteomic and phosphoproteomic analyses is outlined in Figure 1. We identified 14209 peptides (Table S-1) corresponding to 2709 proteins (Table S-2), of which 627 proteins were found to be differentially expressed among the two strains as per the arbitrary minimum cutoff of two-fold change (Figure 2A). Of the 2709 proteins, 2698 proteins were identified in proteomic analysis. An additional 11 proteins were identified uniquely in the phosphoproteomic analysis. Using PhosphoRS probability cutoff of >75%, we identified 512 phosphosites mapping to 257 proteins of *M. tuberculosis* (Table S-3a), 417 of which were nonredundant and unique phosphorylation sites (Figure 2B). Of the 257 proteins, 243 proteins were found to be phosphorylated at a single site on protein sequence, and 14 proteins were phosphorylated at two or more sites. As expected, in line with previously published reports, we observed the distribution of phosphorylation to be highest on threonine residues (68%) followed by serine (29%) and tyrosine residues (3%). The overall difference and overlap in differentially expressed

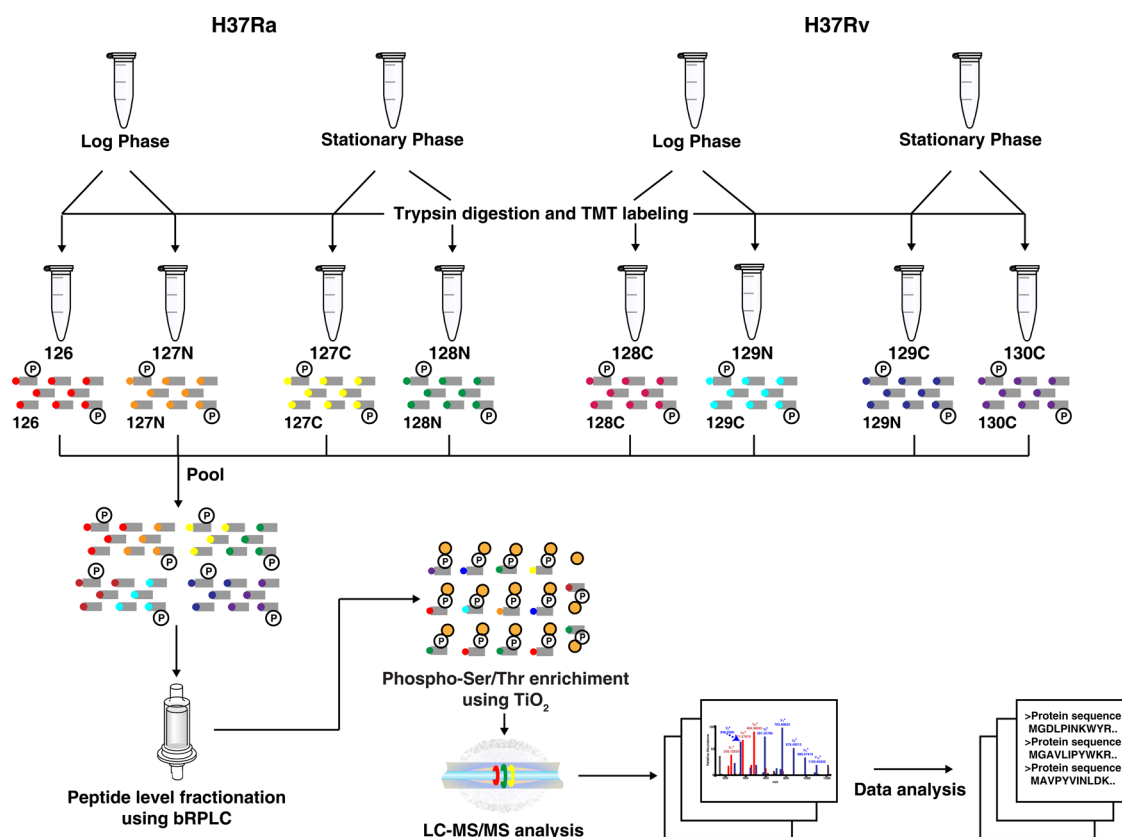


Figure 1. Schematic workflow for quantitative proteomic and phosphoproteomic analysis of H37Ra and H37Rv strains of *M. tuberculosis*. The cultures were harvested at the indicated phases, and protein samples were digested with trypsin followed by TMT labeling. Samples were pooled after bRPLC fractionation and phosphopeptides were enriched using TiO₂ beads. The resulting samples were analyzed on an Orbitrap Fusion mass spectrometer.

proteins between the two strains and growth phases is shown in Figure 2C.

Comparison of our findings with previously published mycobacterial phosphoproteomic studies revealed 265 novel and 152 previously known phosphosites from *M. tuberculosis*. Of the 215 phosphorylation sites reported by Prusic et al., we identified 102 phosphorylation sites in common (Table S-3b). Furthermore, we also identified high-confident localization for 75 phosphorylation sites that have been reported as ambiguous phosphosites in the previous study.⁸ Similarly, 117 phosphorylation sites were found to be common to phosphorylation sites identified in *M. tuberculosis* Beijing isolate, and 13 sites were found to be common to *M. bovis*^{10,11} (Figure 2D). Although we did not specifically enrich for phosphotyrosine modifications, we observed nine novel phosphotyrosine sites in our study when compared to those in a previous phosphotyrosine analysis of *M. tuberculosis*.¹⁷

Protein phosphorylation is an important mechanism involved in the widespread regulation of cellular function. Levy et al., have shown that the protein abundance correlated with the level of phosphorylation.^{18,19} We calculated Pearson's correlation coefficient to determine the correlation between phosphorylation levels and protein abundance for the proteins identified in our study. The analysis revealed correlation between the two, with a correlation coefficient (r) of 0.6 (Figure 3).

Enrichment Analysis Revealed Pathways Enriched for Virulence

Studies have shown that *M. tuberculosis* switches different metabolic pathways to consume fatty acids in place of carbohydrates during persistent infection.^{19,20} Further, the lipid composition of

bacterial cell wall may contribute to virulence.²¹ Using microarray technology, Gao et al., have shown that genes involved in lipid metabolism and cell wall synthesis were enriched in H37Rv when compared with H37Ra. This indicates that the cell wall and cell membrane may be major sites for differences between the two strains.²² It has also been previously reported that the two-component regulatory system and bacterial secretion system play an important role in mycobacterial virulence.^{23,24} We performed network analysis using DAVID Bioinformatics Resources 6.7¹⁶ and identified the enrichment of pathways that belonged to (i) two-component system, (ii) oxidative phosphorylation, (iii) bacterial secretion system, and (iv) fatty acid biosynthesis and ribosomal proteins related pathways. We identified the highest enrichment of ribosomal proteins with a total representation of 44 proteins. Proteomic expression patterns of most of the 30S ribosomal proteins identified (e.g., Rps J-N1) were found to be overexpressed by more than two-fold in the log phase of H37Rv when compared with H37Ra log phase. In this category, the phosphorylation pattern of RpsD was also found to be up-regulated in H37Rv log phase. *M. tuberculosis* uses various secretion systems to secrete proteins, which are essential for mycobacterial virulence or viability.²⁵ We observed differential expression and phosphorylation of several bacterial secretion system-associated proteins among the two strains.

Alterations in Virulence Associated Type VII Secretion System

Type VII secretion system, also known as T7SS, encodes for several virulence associated genes in *M. tuberculosis*. ESAT-6 and CFP-10, secreted by T7SS, have been earlier described as dominant antigens recognized by T-cells in humans and bovine.^{26,27}

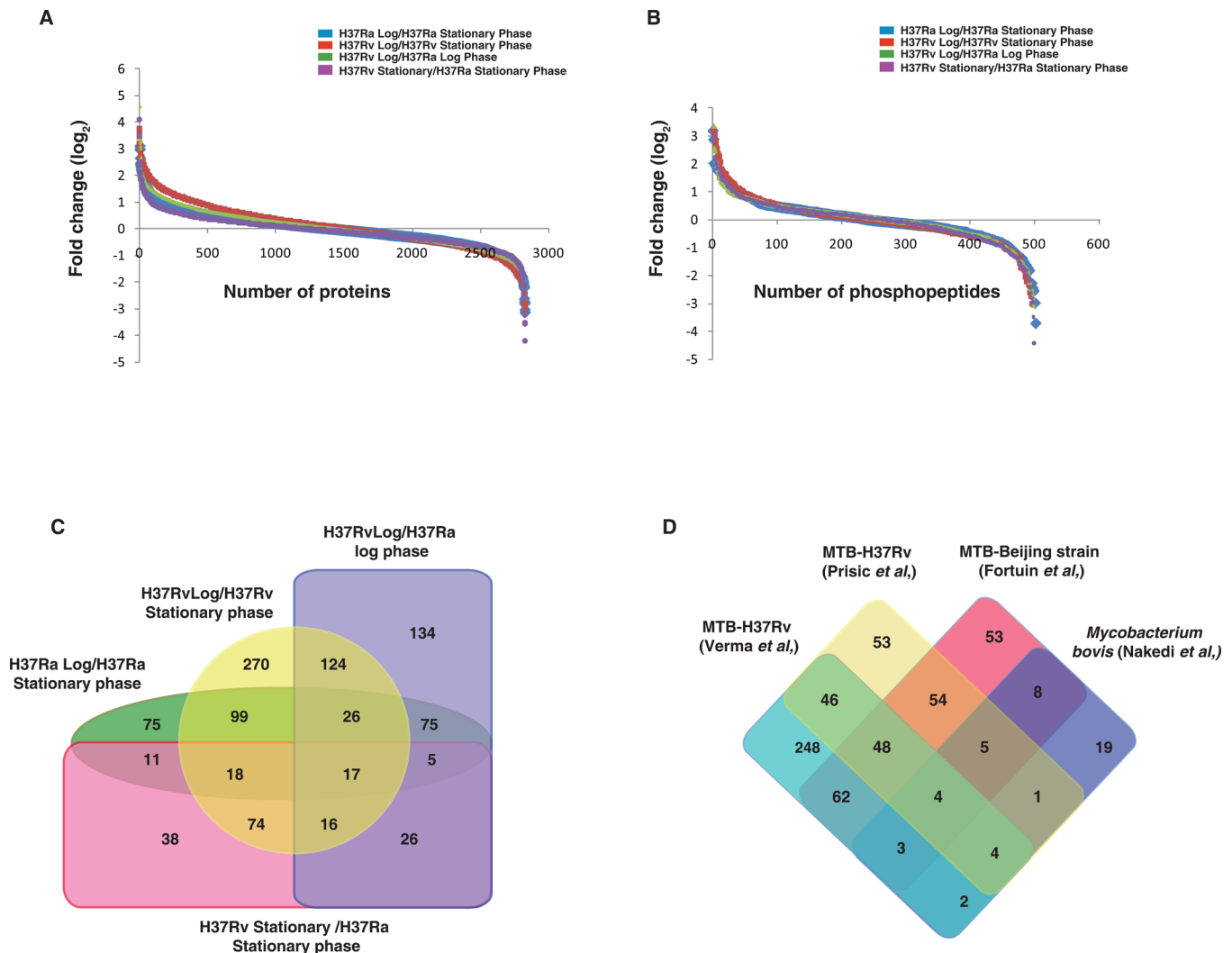


Figure 2. (A) Distribution of \log_2 -transformed ratios (H37Ra Log/H37Ra Stationary phase, H37Rv Log/H37Rv Stationary phase, H37Rv Log/H37Ra Log phase, and H37Rv Stationary/H37Ra Stationary phase) of all proteins identified in the total proteome analysis. (B) Distribution of \log_2 -transformed phosphopeptide ratios (H37Ra Log/H37Ra Stationary phase, H37Rv Log/H37Rv Stationary phase, H37Rv Log/H37Ra Log phase, and H37Rv Stationary/H37Ra Stationary phase) of all the phosphorylated proteins identified in the analysis. (C) Overall difference and overlap between the two strains and growth phases in differentially expressed proteome. (D) Overall difference and overlap between H37Ra and H37Rv strain of *M. tuberculosis* compared with the published phosphoproteomic data from *M. tuberculosis* H37Rv strain, *M. tuberculosis* Beijing strain, and *M. bovis*.

Genes encoding these antigens are located on Region of difference1 (RD1) a 9.5 kb fragment absent in *M. bovis* BCG strain.²⁸ Jhingan *et al.*, in an ESAT-6 antibody based treatment of infected THP-1 cell line, have shown that the elevated levels of ESAT-6 protein in *M. tuberculosis* provide survival advantage. We observed a 2.4-fold hyperphosphorylation of CFP-10 in H37Rv log phase in comparison to H37Ra log phase. Two proteins earlier reported to be integral component of membrane and cell wall were found to be overexpressed in H37Rv compared to H37Ra-Rv3615c (EspC) (9.8-fold) and Rv3616c (9.5-fold) (Figure 4). These proteins belong to Rv3614c-Rv3616c gene cluster specific to mycobacteria and close relatives.²⁹ A recent study by Sassetti *et al.*, has demonstrated that mutations in any of these genes result in virulence attenuation in *M. tuberculosis*.³⁰ Studies have also identified Rv3615c as a highly immunodominant antigen in latent and active TB. Additionally, T-cell responses to Rv3615c are highly specific (93%) for *M. tuberculosis* infection suggesting the role of this antigen in TB infection³¹ (Figure 5). Furthermore, we found secretion-associated proteins EspA, EspC, and EspR to be overexpressed more than 5-fold in H37Rv log phase. We also

observed 2.8-fold hyperphosphorylation of EspR protein at S111 in H37Rv log phase when compared with H37Ra log phase.

In addition, proteins associated with two other secretion-associated systems, general secretion pathway (Sec-pathway) and the twin arginine translocation (Tat-pathway), were also identified in our analysis. Sec system is involved in translocation of unfolded proteins across the mycobacterial cell membrane. It is responsible for the secretion of proteins associated with diverse functions such as metabolism, substrate uptake, and cell communication.^{32,33} Tat system on the other hand is involved in transporting folded proteins across the membrane.³⁴ We identified seven proteins involved in Sec secretion system, of which two proteins, SecE1 and SecF1, were found to be phosphorylated in both the strains. SecE2 was more than 2-fold overexpressed in H37Rv log phase when compared with H37Ra log phase. SecE2 had a unique calcium binding site and was involved in sequestering small ligands.³⁵ In Tat system, we identified three major Tat components, TatA, TatB, and TatC. Expression of TatC was found to be elevated in H37Rv log phase when compared with H37Ra log phase. Three phosphosites corresponding to Tata

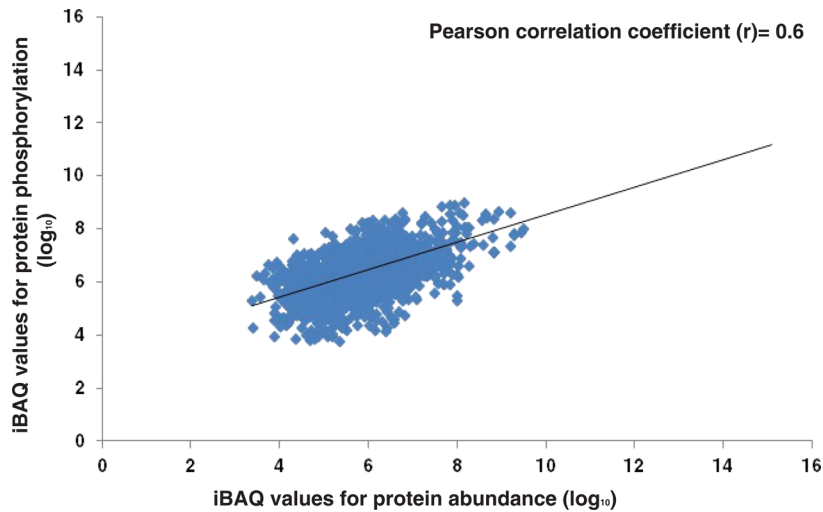


Figure 3. Correlation between phosphorylation level and protein abundance for the proteins identified in the study. For absolute quantification of proteins, iBAQ values were calculated for global proteome and phosphoproteome data.

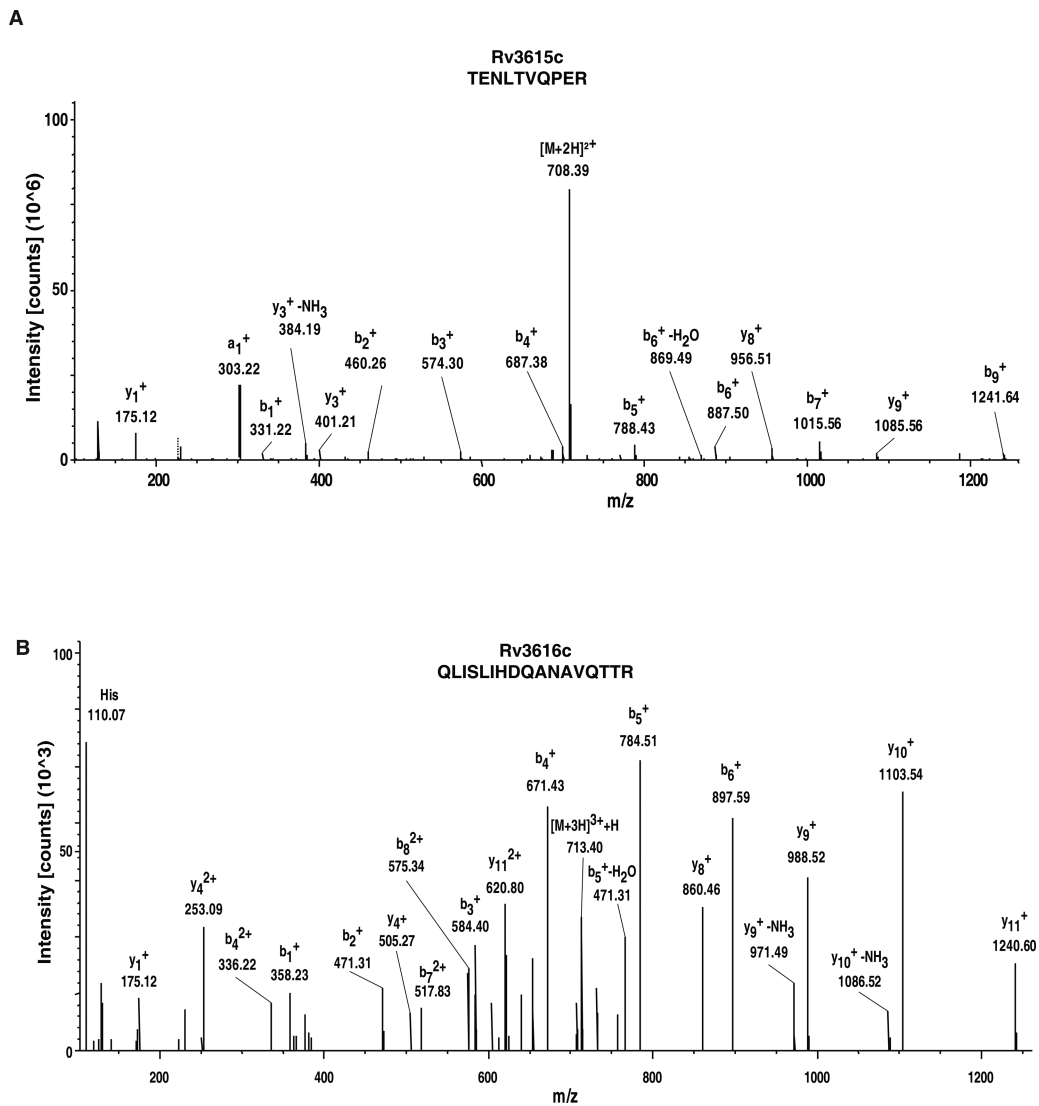


Figure 4. Representative MS/MS spectra depicting two proteins, Rv3615c and Rv3616c, overexpressed in H37Rv compared to H37Ra (A) ESX-1 secretion-associated protein EspC (Rv3615c) (9.8-fold), (B) ESX-1 secretion-associated protein EspA (Rv3616c) (9.5-fold).

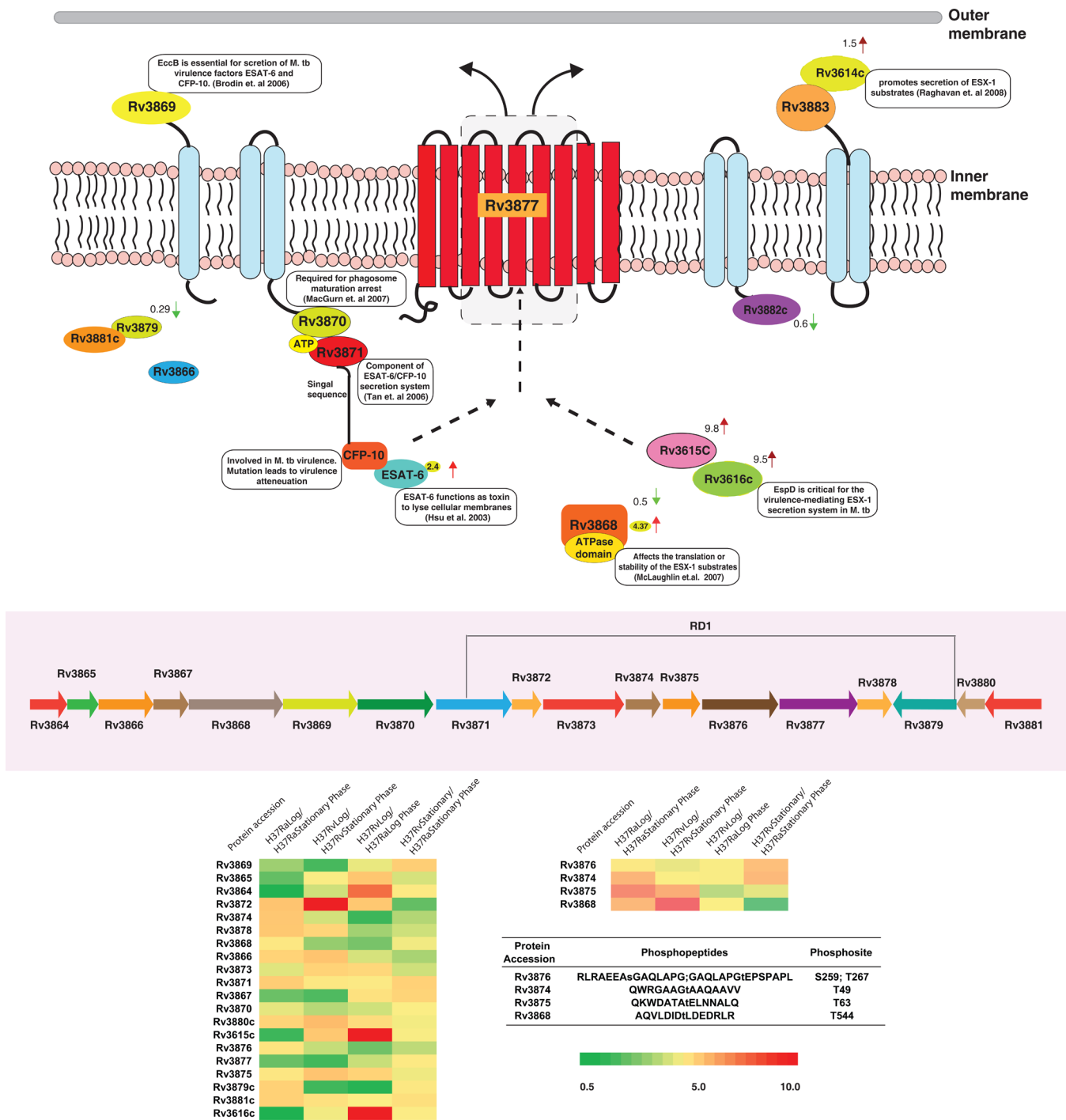


Figure 5. Type VII secretion system in *M. tuberculosis*. Proteins that are upregulated in H37Rv log phase with respect to H37Ra log phase are represented with red arrow. Proteins downregulated are represented as green arrow. Yellow circle is used for representing the phosphorylated proteins. The level of expression or phosphorylation of proteins is represented in heat map.

protein were found to be phosphorylated in our study in both the strains, of which T60 on Tat protein was more than 3-fold hyperphosphorylated in H37Ra log phase than H37Rv log phase. Overall, our data suggest that proteins with altered expression and phosphorylation identified in this study may have important biological roles in infection and virulence of *M. tuberculosis*.

Differential Expression and Phosphorylation of Proteins between H37Ra and H37Rv Strains during Log and Stationary Phases

We observed differential expression and phosphorylation of proteins within and among the two strains at log and stationary

growth phases (p -value ≤ 0.05) (Table S-1 and Table S-3a). In H37Ra strain, 325 proteins were differentially expressed, whereas in virulent H37Rv strain, 649 proteins were found to be differentially expressed. Between the log phases of H37Rv and H37Ra, 240 proteins were overexpressed and 183 proteins were downregulated in H37Rv. We also observed alterations in the level of expression in H37Rv and H37Ra stationary phase. In all, 204 proteins showed altered expression pattern. Eighty-two proteins were overexpressed and 122 proteins were downregulated in H37Rv stationary phase when compared with H37Ra stationary phase.

Interestingly, eight proteins, Rv1766, GlnB, PE15, Rv0141c, Rv3175, Cyp141, DrrB, and TatC, were not expressed in one of the stages among the two strains. For instance, ABC transporter permease DrrB, which is involved in active transport of antibiotic and phthiocerol dimycocerosate (Dim) across the membrane,³⁶ was not expressed in H37Rv log phase. On the contrary, Rv1766, Cyp141, and TatC were not expressed in H37Rv stationary phase.

We also observed differences at phosphorylation levels between the two strains at log and stationary phases. Of the 417 unique phosphorylation sites identified in our study, phosphorylation patterns of 152 phosphorylation sites on 94 proteins were found to be differential (arbitrary minimum cutoff of two-fold change) across the two strains in log and stationary phases. Fifty-five phosphosites were hyperphosphorylated and 97 hypophosphorylated in virulent H37Rv strain as compared to avirulent H37Ra strain.

Using label-free quantification analysis, Jhingan et al., have recently compared the proteome of H37Ra, H37Rv, and *M. tuberculosis* clinical isolates.³⁷ The analysis led to the identification of 2161 proteins, of which we identified 1990 proteins in common. Several proteins were downregulated in H37Ra including Rv3085 (oxidoreductase), acyl carrier protein AcpA, and esterase/lipase LipF. We also observed a similar trend in H37Ra protein expression suggesting the role of these proteins in changed phenotype of H37Ra. Upregulation of Esx family proteins was also observed in H37Rv and *M. tuberculosis* clinical isolates.³⁷ Esx proteins are known to be associated with virulence of *M. tuberculosis*. The level of expression can be correlated with increased virulence in clinical isolates as observed in the JAL clinical isolate.³⁸ We further observed upregulation of Rv1446 (OpcA) and Rv2145c (Wag31) in H37Rv log phase compared to H37Ra log phase. Additionally, we also observed hyperphosphorylation of Wag31 in H37Rv compared with H37Ra strain. These proteins have been previously reported to be expressed at higher levels in *M. tuberculosis* isoniazid drug resistant strains³⁷ and are known to be involved in peptidoglycan biosynthesis and oxidative stress.^{39,40} Altered phosphorylation and expression of these proteins therefore implicate their role in pathogenesis.

Functional Classification of the Identified Proteins Reveals Marked Differences between the Two Strains

To determine whether proteins that are differentially represented in any particular cellular process, Gene Ontology enrichment analysis for differentially expressed and differentially phosphorylated proteins was performed using PANTHER classification system.⁴¹ The comparison was done within the individual strain and between the two strains across log and stationary phases. Significantly enriched cellular processes (p -value ≤ 0.05) among differentially expressed/phosphorylated proteins are provided in Figure S-1.

Previous studies on comparative genomics of H37Ra and H37Rv strains have reported SNVs and indels in PE/PPE/PE-PGRS gene family that led to gross genetic changes.³ It has been previously reported that certain members of this gene family impact the process of antigen presentation and involved in generating antigenic diversity.⁴² We observed 24-fold overexpression and four-fold hyperphosphorylation of PE family protein PE31 in H37Rv log phase when compared with H37Ra. We also found 4.5-fold overexpression of extracellular region protein PE15 (Rv1386) in H37Rv log phase when compared with H37Ra log phase. PE15 is known to evade the host immune

response and favor in vivo survival of bacteria.⁴³ Additionally, we found 12-fold overexpression of PE15 protein in H37Rv log phase when compared with H37Rv stationary phase. PE15 on the other hand was not expressed in H37Ra stationary phase. This suggests that the transmembrane proteins may play a potential role in virulence.

We identified six major clusters of proteins, which showed considerable changes in phosphorylation patterns between two strains across log and stationary phases. The trend in the phosphorylation pattern across various stages and between the two strains is represented in heat map (Figure 6). Many of the

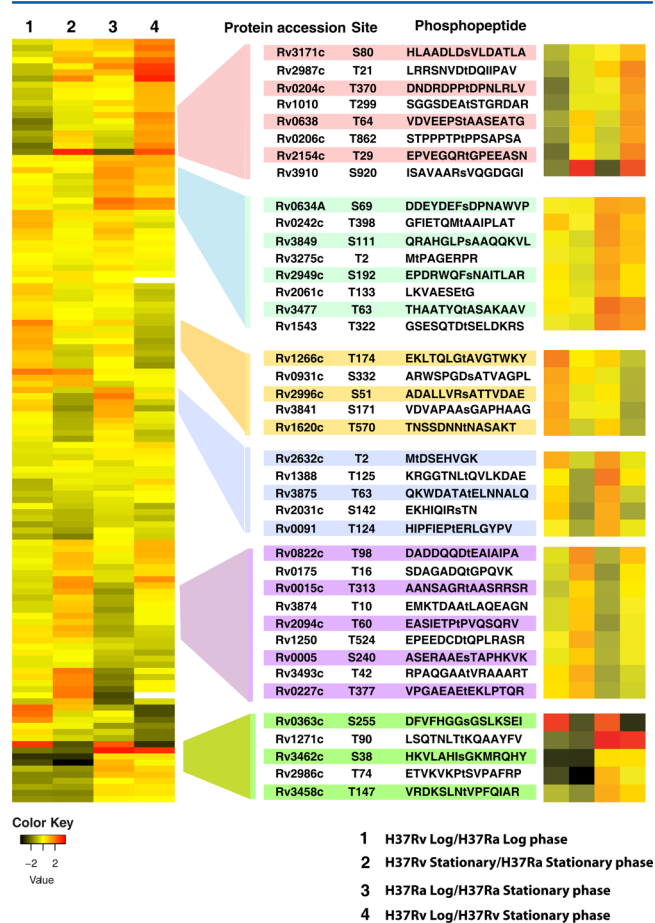


Figure 6. Heat map depicting phosphorylation changes in H37Ra and H37Rv strains of *M. tuberculosis* across log and stationary growth phases. A global color gradient ranging between green for proteins with fold change ≤ 0.5 to yellow for values between 0.6 and 2 and red for values ≥ 2.0 was applied on the clustered data set.

proteins falling in these clusters, including EspR, FabG4, and Rv1543, are known to be involved in protein secretion, fatty acid biosynthesis, and fatty acid oxidation, respectively.^{44–46} Interestingly, we observed more than 2-fold hyperphosphorylation of chaperonin GroEL2 and chaperonin GroES in the stationary phase of H37Rv without any significant changes in their expression levels. GroEL is an essential chaperonin and is responsible for cellular processes such as de novo folding and macromolecular assembly. Immunochemical and mass spectrometry-based analyses have shown that GroEL1 exists in multiple forms. The switch between single ring and double ring oligomer is controlled by phosphorylation of GroEL indicating the role of phosphorylation in activity of GroEL.⁴⁷ Regulated oligomerization between the *M. tuberculosis* chaperonin helps in controlled

utilization of ATP under suboptimal nutrient conditions,⁴⁸ which suggests its role in persistence of *M. tuberculosis* in host cell. Furthermore, immunity and pathogenicity to *M. tuberculosis* infection in the host are mediated by the recognition of a range of mycobacterial antigens. GroEL2 is one such antigen, originally identified as a highly immunoreactive protein in *M. leprae* extracts.⁴⁹ This candidate class of GroEL (cpn60 or Hsp60) molecular chaperones contain epitopes shared among various species of mycobacteria. However, their phosphorylation pattern(s) has been suggested to be species dependent.⁵⁰ Described as an essential gene for *in vitro* growth of H37Rv,⁵¹ GroEL2 protein levels have been reported to be upregulated in response to multiple conditions.^{52–54} This protein is a substrate of *M. tuberculosis* STPKs *in vitro*.^{49,54} In the current study, we observed phosphorylation of GroEL at T47, T49, S54, and T479. Interestingly, all the four sites were hyperphosphorylated in H37Rv stationary phase as compared to that of H37Ra. Apart from their conventional roles, chaperones have been predicted to serve as immunodominant antigens upon infection in the host.²⁸ Rv3269 is another protein with predicted chaperoning activity that showed altered expression between virulent and avirulent strains. Although described as a nonessential gene,⁵¹ it is required for bacterial survival in primary murine macrophages. Phosphorylation pattern of this protein was also found to be altered across the growth stages of H37Ra and H37Rv. We also observed 3.8-fold hyperphosphorylation of integration host factor MihF in

log phase of H37Rv when compared with log phase of H37Ra. Furthermore, we observed 5.5- and 7.6-fold hyperphosphorylation at S255 in fructose-bisphosphate aldolase protein at H37Rv log and stationary phase, respectively, when compared with that of H37Ra.

Proteases or peptidases have been shown to play an important role in the virulence and pathobiology of infectious microorganisms.^{55–57} *M. tuberculosis* has more than 100 genes encoding proteases or peptidases.⁵⁵ We identified 28 proteases including PpepA, HtpX, PepR, and ClpC2. Probable zinc protease PepR belongs to peptidase family M16. This protease is required by *M. tuberculosis* for its survival and pathogenicity.⁵⁸ We observed 2-fold downregulation of PepR in H37Rv stationary phase when compared with H37Ra stationary phase. Membrane-associated serine protease (Rv3671c) was found to be downregulated by 0.5-fold in the log phase of H37Rv when compared to H37Ra log phase.

A partial set of other differentially expressed or phosphorylated among the two strains in log and stationary phases is provided in Tables 1 and 2.

M. tuberculosis Kinome Reveals Differential Expression and Phosphorylation Patterns across the Growth Phases in Their Substrates

The activities of cellular kinases and phosphatases are often regulated through post translational modifications (PTMs). We identified all 11 known STPKs of *M. tuberculosis*, of which

Table 1. List of Differentially Phosphorylated Proteins among Two Strains That Are Known To Play an Important Role in Virulence or Pathogenesis of *M. tuberculosis*

protein ID	description	H37Ra Log/ H37Ra Stationary	H37Rv Log/ H37Rv Stationary	H37Rv Log/ H37Ra Log	H37Rv Stationary/ H37Ra Stationary
Rv0163	acyl-CoA thioester hydrolase	1.0	2.9	3.1	1.1
Rv3864	ESX-1 secretion-associated protein EspE	0.3	0.8	2.7	0.9
Rv2031c	heat shock protein HspX	0.4	0.1	1.0	3.1
Rv3822	membrane-associated acyltransferase	1.1	1.2	3.7	3.2
Rv0981	mycobacterial persistence regulator MRPA	0.9	1.7	2.0	1.1
Rv3085	oxidoreductase	0.6	3.4	10.3	2.0
Rv3477	PE family protein PE31	0.5	1.0	24.3	11.1
Rv3161c	oxidoreductase	0.3	3.6	8.2	0.7
Rv0033	acyl carrier protein AcpA	1.3	7.7	4.5	0.8
Rv0077c	oxidoreductase	0.7	3.2	4.5	0.9
Rv1397c	Toxin VapC10	0.8	2.0	4.3	1.7
Rv0299	toxin	1.1	3.7	4.1	1.2
Rv2775	N-acetyltransferase	0.2	2.1	4.0	0.4

Table 2. List of Important Virulence Associated Proteins Differentially Expressed or Phosphorylated among the Two Strains in Log and Stationary Phase

protein ID	description	phosphosite in protein	H37Ra Log/ H37Ra Stationary	H37Rv Log/ H37Rv Stationary	H37Rv Log/ H37Ra Log	H37Rv Stationary/ H37Ra Stationary
Rv3477	PE family protein PE31	T63	1.0	3.2	4.2	1.3
Rv2154c	cell division protein FtsW	T29	1.3	3.4	0.6	0.2
Rv0933	phosphate-transport ABC transporter ATP-binding protein PstB	S266	1.0	1.0	4.4	4.2
		S252	0.6	0.6	1.7	1.6
Rv3817	aminoglycoside 3'-phosphotransferase	S250	2.8	6.2	2.6	1.2
Rv1271c	hypothetical protein	T90	0.2	8.1	10.2	0.3
Rv1388	integration host factor MihF	T125	0.4	1.3	3.8	1.2
		T169	0.8	1.6	1.7	0.9
		S189	1.6	5.5	2.1	0.6
Rv1543	fatty-acyl-CoA reductase	T322	0.7	2.8	3.5	0.9
Rv3849	ESX-1 secretion-associated regulator EspR	S111	0.7	1.9	2.8	1.0
Rv2949c	early secretory antigenic target EsxA	S192	0.7	1.4	2.5	1.3
Rv3875	early secretory antigenic target EsxA	T63	0.4	0.6	2.5	1.6

six were found to be phosphorylated. For most of the kinases, threonine was identified as preferred phosphoreceptor residue and was in accordance with earlier studies on *M. tuberculosis*.^{8–10} PknA is essential for the survival of the pathogen in the host and phosphorylation in its activation loop has been reported to be pivotal for bacterial growth.⁵⁹ Transcript accumulation of PknB has been previously demonstrated during bacterial growth in alveolar macrophages,⁶⁰ whereas its protein level was reported to be down-regulated under conditions of nutrient starvation,⁶¹ indicating its role in bacterial growth. We observed decreased phosphorylation (0.4-fold) in PknA T313 residue in H37Rv when compared with H37Ra. PknD, like PknA and PknB, is a transmembrane STPK with autophosphorylatable threonine residues. We observed hyperphosphorylation at T277 and S332 in H37Rv stationary phase. An increased level of phosphorylation of PknD may be correlated with its requirement for bacterial survival inside host. *M. tuberculosis* protein kinase PknH, described previously as a nonessential gene⁶² and reported to be present only in H37Rv-infected guinea pig lungs at 90 days and not 30 days,⁶³ was found to be 3.5-fold hyperphosphorylated in H37Rv stationary phase. Three mycobacterial kinases, PknA, PknD, and PknH, identified in our analysis shared several substrates such as FhaA, MmpL3, and Rv3910.⁸ These substrates have been previously reported to be involved in signal transduction,⁴⁵ lipid biosynthesis,^{62,64} and hypophosphorylation of all the three proteins and were observed in H37Rv indicating the role of phosphorylation in regulating mycobacterial signaling and metabolism.

In addition, our data also revealed expression of protein kinases involved in the two-component signal transduction pathway. Sensor-type histidine kinase PrrB and sensor histidine kinase MtrB showed differential expression between the two strains. These kinases are part of two-component signaling and are known to play an important role in mycobacterial virulence and pathogenesis.^{23,24} The pathway essentially consists of a membrane bound sensor kinase (that contains an autophosphorylatable histidine residue) and a response regulator (with a phosphorylatable aspartate) that transmits the signals downstream. Two-component regulatory proteins act as sensory and adaptive factors in response to a wide range of environmental stimuli. PhoP/PhoQ two component system controls transcription of virulence genes essential for survival of *M. tuberculosis* in host cells.⁶⁵ We observed 2-fold overexpression of PhoP in H37Rv stationary phase compared with H37Ra stationary phase.

A remarkable number of kinases (ThiD, IspE, PknH, CysN, PfkB, PfkA, and GlpK) were observed to be downregulated in H37Rv log phase when compared with H37Ra log phase. All these kinases except for PknH are involved in various metabolic processes.^{51,66,67} PfkA, PfkB, and GlpK are all involved in central C metabolism,^{68,69} ThiD is involved in thiamine synthesis,⁵¹ and IspE is annotated to be involved in isoprenoid biosynthesis.⁶² Downregulation of key metabolic enzymes between virulent and avirulent strains suggests that virulence may also be linked to nutrient sensing and metabolized by the intracellular pathogen.⁷⁰ An opposite trend was observed for PyrH, which showed an upregulation pattern in H37Rv compared to H37Ra. This protein was earlier reported to be specific to H37Rv when compared with two attenuated strains of *M. tuberculosis*.²⁶ Our data also suggest that proteins reported earlier as missing/absent in a given strain were actually low abundant and not identified during previous analyses. High-resolution mass spectrometry enabled us to identify and quantify these proteins in both the strains.

Phospho-Motif Analysis of Differentially Phosphorylated Proteins in H37Ra and H37Rv Strains

To gain insight into the potential categorization of mycobacterial kinase substrates, which are differentially phosphorylated among H37Ra and H37Rv strains, we performed phospho-motif analysis using Motif-X algorithm.¹⁵ We identified predominantly three phospho-motifs, EXXpT, PpT, and pTXp (Figure 7). Twenty-one

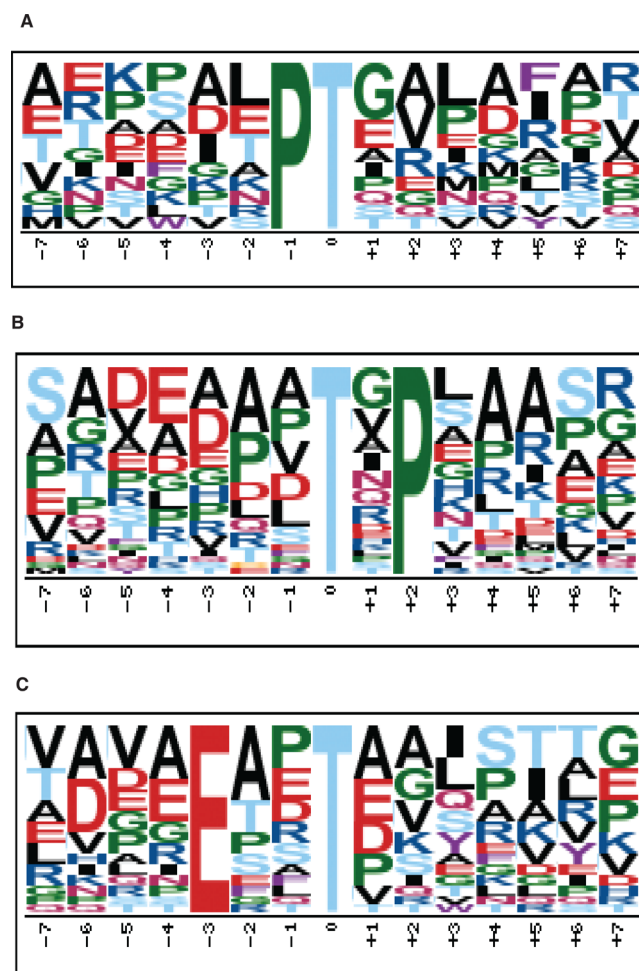


Figure 7. Phosphorylation site motif analysis using differentially phosphorylated proteins for the mycobacterial kinase substrates in H37Ra and H37Rv strains. Weblogo A, B, and C generated using Motif-x algorithm. The motifs show the relative statistical significance of the logo generated with respect to *M. tuberculosis* background.

substrates shared EXXpT motif, of which nine proteins were hypophosphorylated in H37Rv log phase and four proteins were hyperphosphorylated in H37Rv stationary phase. In this category, the MmpL3 protein involved in lipid metabolism was found to be five-fold hypophosphorylated in H37Rv. Furthermore, we observed hyperphosphorylation in 7 out of 14 proteins in H37Rv sharing PpT motif. Interestingly, 28 kinase substrates shared pTXp, of which nine were hypophosphorylated in H37Rv stationary phase. Most of the proteins that vary in phosphorylation in this category belonged to cell wall or cell membrane component. It has been previously shown that cell wall and cell membrane play an important role in virulence of mycobacterium.⁷¹

Differences in Growth Phases and Their Significance in Tuberculosis Pathogenesis

One of the important aspects of tuberculosis pathogenesis is latency stage where *M. tuberculosis* maintains an asymptomatic

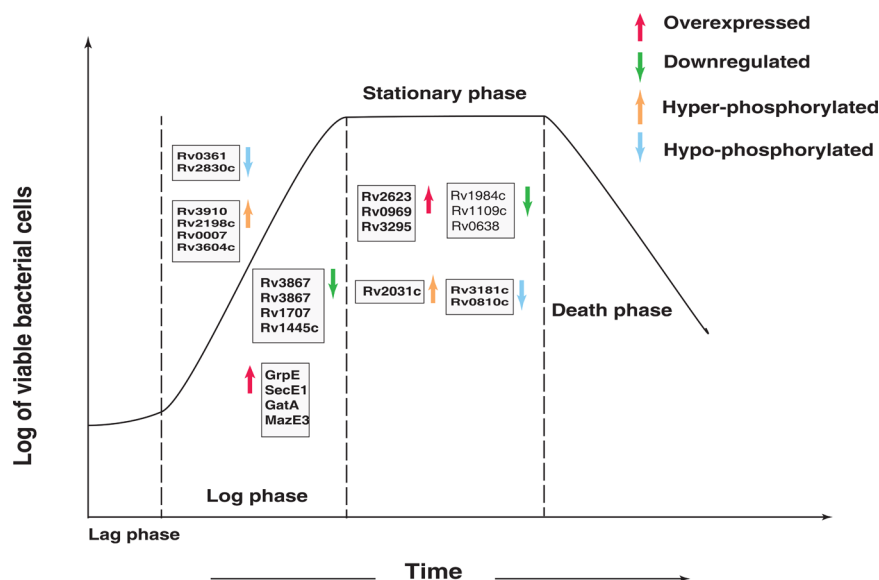


Figure 8. Growth phase-specific expression and phosphorylation of proteins in both H37Ra and H37Rv strains.

state in the host. The majority of tuberculosis cases result due to reactivation of latent bacteria, which are quiescent within the host. Studies on tuberculosis pathogenesis suggest that initial event of mycobacterial infection involves entry in macrophage followed by rapid growth phase and granuloma formation.^{72–74} The bacilli attain stationary phase inside primary granuloma. The environment inside granuloma, such as low pH, low oxygen, and nutrients, toxic oxygen species directs mycobacteria toward dormancy. Studies have shown that actively dividing bacteria at their log phase are killed at the beginning of antitubercular therapy. However, bacteria in their stationary, nonreplicating stage have reduced susceptibility to antitubercular drugs. These bacteria usually require a prolonged treatment for complete pathogen clearance.⁷⁵ Moreover, it has been previously shown that in vitro-grown *M. tuberculosis* that has reached stationary phase is more resistant to high temperature than exponentially growing bacteria.⁷⁶ Several studies have earlier demonstrated increased tolerance to stress in stationary phase of *M. tuberculosis*.⁷⁷ Efforts to identify proteomic changes specific to log and stationary phase would allow better understanding of latency and *M. tuberculosis* pathogenesis. We identified 81 proteins overexpressed only in log phase of both H37Ra and H37Rv strains irrespective of their virulence properties. Fifty proteins on the other hand were overexpressed only in stationary phase of both the strains suggesting the role of these proteins in different growth phases of mycobacteria. Interestingly, we observed overexpression of Universal stress protein-Rv2623 in stationary phase of both the strains. This protein is a member of the dormancy regulon and is known to be induced in hypoxia and low levels of nitric oxide.^{68,69} Additionally, we identified four proteins, GrpE, SecE1, GatA, and MazE3, overexpressed in log phase. These proteins are known to play an important role in bacterial growth.⁵¹ We also observed hyper-phosphorylation of four proteins, Rv3910, Rv2198c, Rv0007, and Rv3604c, which are components of mycobacterial cell wall (Figure 8). Rv3910, an integral membrane protein, was more than five-fold hyper-phosphorylated in H37Ra and H37Rv log phase. This protein in phosphorylated form is known to control cell wall synthesis.⁷⁸ Differences in proteome expression and phosphoproteomic profiles at log and stationary phases indicate their association in switching from one growth phase to another.

The candidate molecules identified in the current study may further be considered for growth-specific studies in *M. tuberculosis*.

CONCLUSIONS

Through phosphoproteomic profiling of virulent and avirulent strains of *M. tuberculosis* at different growth phases, we demonstrate that the two strains are highly similar at protein level. However, marked differences between the two strains at expression levels and phosphorylation patterns could be responsible for the difference in their phenotypes. Significant differences in protein expression and phosphorylation in PE/PPE/PE–PGRS gene family further support the genomic findings reported earlier. Our results clearly indicate that not only the proteins involved in pathways pertaining to bacterial virulence and pathogenesis are affected, but also pathways for lipid metabolism and ribosomal proteins that are involved in various metabolic processes are dysregulated. This suggests that there are hitherto unknown mechanisms that control the virulence and pathogenesis of *M. tuberculosis* inside host cell. Our data provide a valuable resource for investigating signaling pathways that regulate pathogenesis in *M. tuberculosis*.

ASSOCIATED CONTENT

Supporting Information

The Supporting Information is available free of charge on the ACS Publications website at DOI: 10.1021/acs.jproteome.6b00983.

Gene Ontology enrichment analysis for differentially expressed or phosphorylated proteins using PANTHER classification system (PDF)

List of peptides identified by LC–MS/MS analysis of H37Ra and H37Rv strains of *M. tuberculosis* at log and stationary phase (XLSX)

List of proteins identified by LC–MS/MS analysis of H37Ra and H37Rv strains of *M. tuberculosis* at log and stationary phase compared with list of proteins identified in earlier studies (XLSX)

List of phosphopeptides identified in H37Ra and H37Rv strains at log and stationary phase (XLS)

List of phosphopeptides identified in H37Ra and H37Rv strains at log and stationary phase that were earlier identified in *M. bovis*, *M. smegmatis*, and *M. tuberculosis* Beijing strains (XLS)

AUTHOR INFORMATION

Corresponding Authors

*E-mail: sheetal.gandotra@igib.in.

*E-mail: keshav@ibioinformatics.org. Phone: +91 80 28416140.

ORCID

Thottethodi Subrahmanya Keshava Prasad: 0000-0002-6206-2384

Notes

The authors declare no competing financial interest.

The mass spectrometry proteomics data were deposited to the ProteomeXchange Consortium (<http://proteomecentral.proteomexchange.org>) via the PRIDE partner repository with the data set identifier PXD004161.

ACKNOWLEDGMENTS

T.S.K.P. is the recipient of the DST-IDP research grant “Development of epitope based diagnostic gadget for detection of *M. tuberculosis* in the Indian population” from the Department of Science Technology, Government of India. We thank the Department of Biotechnology (DBT), Government of India and Infosys Foundation for research support to the Institute of Bioinformatics. We thank Ministry of Health and Family Welfare, Government of India for procuring Orbitrap Fusion instrument at NIMHANS-IOB laboratory. S.M.P. is a recipient of INSPIRE Faculty Award from Department of Science and Technology (DST), Government of India. R.V. and G.D. are recipients of Senior Research Fellowship from University Grants Commission (UGC), Government of India. J.A. and M.K. are recipients of Senior Research Fellowship from Council of Scientific and Industrial Research (CSIR), Government of India. S.G. is a Wellcome Trust/DBT India Alliance Intermediate Fellow.

ABBREVIATIONS

TMT, tandem mass tag; BLAST, Basic Local Alignment Search Tool; ETD, electron transfer dissociation; PSM, peptide spectrum match; FDR, false discovery rate; PTM, post-translational modification

REFERENCES

- (1) Broset, E.; Martin, C.; Gonzalo-Asensio, J. Evolutionary landscape of the Mycobacterium tuberculosis complex from the viewpoint of PhoPR: implications for virulence regulation and application to vaccine development. *mBio* **2015**, *6* (5), e01289-15.
- (2) Gonzalo-Asensio, J.; Soto, C. Y.; Arbues, A.; Sancho, J.; del Carmen Menendez, M.; Garcia, M. J.; Gicquel, B.; Martin, C. The Mycobacterium tuberculosis phoPR operon is positively autoregulated in the virulent strain H37Rv. *J. Bacteriol.* **2008**, *190* (21), 7068–78.
- (3) Zheng, H.; Lu, L.; Wang, B.; Pu, S.; Zhang, X.; Zhu, G.; Shi, W.; Zhang, L.; Wang, H.; Wang, S.; Zhao, G.; Zhang, Y. Genetic basis of virulence attenuation revealed by comparative genomic analysis of Mycobacterium tuberculosis strain H37Ra versus H37Rv. *PLoS One* **2008**, *3* (6), e2375.
- (4) Sampson, S. L. Mycobacterial PE/PPE proteins at the host-pathogen interface. *Clin. Dev. Immunol.* **2011**, *2011*, 497203.
- (5) Singh, P. K.; Saxena, R.; Tiwari, S.; Singh, D. K.; Singh, S. K.; Kumari, R.; Srivastava, K. K. RD-1 encoded EspJ protein gets

phosphorylated prior to affect the growth and intracellular survival of mycobacteria. *Sci. Rep.* **2015**, *5*, 12717.

- (6) Vilcheze, C.; Molle, V.; Carrere-Kremer, S.; Leiba, J.; Mourey, L.; Shenai, S.; Baronian, G.; Tufariello, J.; Hartman, T.; Veyron-Churlet, R.; Trivelli, X.; Tiwari, S.; Weinrick, B.; Alland, D.; Guerardel, Y.; Jacobs, W. R., Jr.; Kremer, L. Phosphorylation of KasB regulates virulence and acid-fastness in Mycobacterium tuberculosis. *PLoS Pathog.* **2014**, *10* (5), e1004115.

- (7) Corrales, R. M.; Molle, V.; Leiba, J.; Mourey, L.; de Chastellier, C.; Kremer, L. Phosphorylation of mycobacterial PcaA inhibits mycolic acid cyclopropanation: consequences for intracellular survival and for phagosome maturation block. *J. Biol. Chem.* **2012**, *287* (31), 26187–99.

- (8) Prsic, S.; Dankwa, S.; Schwartz, D.; Chou, M. F.; Locasale, J. W.; Kang, C. M.; Bemis, G.; Church, G. M.; Steen, H.; Husson, R. N. Extensive phosphorylation with overlapping specificity by Mycobacterium tuberculosis serine/threonine protein kinases. *Proc. Natl. Acad. Sci. U. S. A.* **2010**, *107* (16), 7521–6.

- (9) Okhrimenko, A.; Grun, J. R.; Westendorf, K.; Fang, Z.; Reinke, S.; von Roth, P.; Wassilew, G.; Kuhl, A. A.; Kudernatsch, R.; Demski, S.; Scheibenbogen, C.; Tokoyoda, K.; McGrath, M. A.; Raftery, M. J.; Schonrich, G.; Serra, A.; Chang, H. D.; Radbruch, A.; Dong, J. Human memory T cells from the bone marrow are resting and maintain long-lasting systemic memory. *Proc. Natl. Acad. Sci. U. S. A.* **2014**, *111* (25), 9229–34.

- (10) Fortuin, S.; Tomazella, G. G.; Nagaraj, N.; Sampson, S. L.; Gey van Pittius, N. C.; Soares, N. C.; Wiker, H. G.; de Souza, G. A.; Warren, R. M. Phosphoproteomics analysis of a clinical Mycobacterium tuberculosis Beijing isolate: expanding the mycobacterial phosphoproteome catalog. *Front. Microbiol.* **2015**, *6*, 6.

- (11) Nakedi, K. C.; Nel, A. J.; Garnett, S.; Blackburn, J. M.; Soares, N. C. Comparative Ser/Thr/Tyr phosphoproteomics between two mycobacterial species: the fast growing Mycobacterium smegmatis and the slow growing Mycobacterium bovis BCG. *Front. Microbiol.* **2015**, *6*, 237.

- (12) Pinto, S. M.; Nirujogi, R. S.; Rojas, P. L.; Patil, A. H.; Manda, S. S.; Subbannayya, Y.; Roa, J. C.; Chatterjee, A.; Prasad, T. S.; Pandey, A. Quantitative phosphoproteomic analysis of IL-33-mediated signaling. *Proteomics* **2015**, *15* (2–3), 532–44.

- (13) Radhakrishnan, A.; Nanjappa, V.; Raja, R.; Sathe, G.; Chavan, S.; Nirujogi, R. S.; Patil, A. H.; Solanki, H.; Renuse, S.; Sahasrabudhe, N. A.; Mathur, P. P.; Prasad, T. S.; Kumar, P.; Califano, J. A.; Sidransky, D.; Pandey, A.; Gowda, H.; Chatterjee, A. Dysregulation of splicing proteins in head and neck squamous cell carcinoma. *Cancer Biol. Ther.* **2016**, *17* (2), 219–29.

- (14) Selvan, L. D.; Renuse, S.; Kaviyil, J. E.; Sharma, J.; Pinto, S. M.; Yelamanchi, S. D.; Puttamalles, V. N.; Ravikumar, R.; Pandey, A.; Prasad, T. S.; Harsha, H. C. Phosphoproteome of Cryptococcus neoformans. *J. Proteomics* **2014**, *97*, 287–95.

- (15) Chou, M. F.; Schwartz, D. Biological sequence motif discovery using motif-x. *Curr. Protoc. Bioinformatics* **2011**, *13*, 15–24.

- (16) Huang, D. W.; Sherman, B. T.; Lempicki, R. A. Systematic and integrative analysis of large gene lists using DAVID bioinformatics resources. *Nat. Protoc.* **2008**, *4* (1), 44–57.

- (17) Kusebauch, U.; Ortega, C.; Olodart, A.; Rogers, R. S.; Sherman, D. R.; Moritz, R. L.; Grundner, C. Mycobacterium tuberculosis supports protein tyrosine phosphorylation. *Proc. Natl. Acad. Sci. U. S. A.* **2014**, *111* (25), 9265–70.

- (18) Levy, E. D.; Michnick, S. W.; Landry, C. R. Protein abundance is key to distinguish promiscuous from functional phosphorylation based on evolutionary information. *Philos. Trans. R. Soc., B* **2012**, *367* (1602), 2594–606.

- (19) Boshoff, H. I.; Barry, C. E. 3rd. Tuberculosis - metabolism and respiration in the absence of growth. *Nat. Rev. Microbiol.* **2005**, *3* (1), 70–80.

- (20) Schnappinger, D.; Ehrst, S.; Voskuil, M. I.; Liu, Y.; Mangan, J. A.; Monahan, I. M.; Dolganov, G.; Efron, B.; Butcher, P. D.; Nathan, C.; Schoolnik, G. K. Transcriptional Adaptation of Mycobacterium tuberculosis within Macrophages: Insights into the Phagosomal Environment. *J. Exp. Med.* **2003**, *198* (5), 693–704.

- (21) Julian, E.; Roldan, M.; Sanchez-Chardi, A.; Astola, O.; Agusti, G.; Luquin, M. Microscopic cords, a virulence-related characteristic of *Mycobacterium tuberculosis*, are also present in nonpathogenic mycobacteria. *J. Bacteriol.* **2010**, *192* (7), 1751–60.
- (22) Gao, Q.; Kripke, K.; Arinc, Z.; Voskuil, M.; Small, P. Comparative expression studies of a complex phenotype: cord formation in *Mycobacterium tuberculosis*. *Tuberculosis (Oxford, U. K.)* **2004**, *84* (3–4), 188–96.
- (23) Feltcher, M. E.; Sullivan, J. T.; Braunstein, M. Protein export systems of *Mycobacterium tuberculosis*: novel targets for drug development? *Future Microbiol.* **2010**, *5* (10), 1581–97.
- (24) Parish, T.; Smith, D. A.; Roberts, G.; Betts, J.; Stoker, N. G. The senX3-regX3 two-component regulatory system of *Mycobacterium tuberculosis* is required for virulence. *Microbiology* **2003**, *149* (6), 1423–35.
- (25) Houben, E. N.; Korotkov, K. V.; Bitter, W. Take five - Type VII secretion systems of *Mycobacteria*. *Biochim. Biophys. Acta, Mol. Cell Res.* **2014**, *1843* (8), 1707–16.
- (26) Aagaard, C.; Govaerts, M.; Meikle, V.; Gutierrez-Pabello, J. A.; McNair, J.; Andersen, P.; Suarez-Guemes, F.; Pollock, J.; Espitia, C.; Cataldi, A. Detection of bovine tuberculosis in herds with different disease prevalence and influence of paratuberculosis infection on PPDB and ESAT-6/CFP10 specificity. *Prev Vet Med.* **2010**, *96* (3–4), 161–9.
- (27) Ravn, P.; Demissie, A.; Egualde, T.; Wondwosson, H.; Lein, D.; Amoudy, H. A.; Mustafa, A. S.; Jensen, A. K.; Holm, A.; Rosenkrands, I.; Oftung, F.; Olobo, J.; von Reyn, F.; Andersen, P. Human T cell responses to the ESAT-6 antigen from *Mycobacterium tuberculosis*. *J. Infect. Dis.* **1999**, *179* (3), 637–45.
- (28) Qamra, R.; Mande, S. C.; Coates, A. R.; Henderson, B. The unusual chaperonins of *Mycobacterium tuberculosis*. *Tuberculosis (Oxford, U. K.)* **2005**, *85* (5–6), 385–94.
- (29) Gey Van Pittius, N. C.; Gamielien, J.; Hide, W.; Brown, G. D.; Siezen, R. J.; Beyers, A. D. The ESAT-6 gene cluster of *Mycobacterium tuberculosis* and other high G+C Gram-positive bacteria. *Genome Biol.* **2001**, *2* (10), research0044.1.
- (30) Sassetti, C. M.; Rubin, E. J. Genetic requirements for mycobacterial survival during infection. *Proc. Natl. Acad. Sci. U. S. A.* **2003**, *100* (22), 12989–94.
- (31) Millington, K. A.; Fortune, S. M.; Low, J.; Garces, A.; Hingley-Wilson, S. M.; Wickremasinghe, M.; Kon, O. M.; Lalvani, A. Rv3615c is a highly immunodominant RD1 (Region of Difference 1)-dependent secreted antigen specific for *Mycobacterium tuberculosis* infection. *Proc. Natl. Acad. Sci. U. S. A.* **2011**, *108* (14), 5730–5.
- (32) Stathopoulos, C.; Hendrixson, D. R.; Thanassi, D. G.; Hultgren, S. J.; St. Geme, J. W., III; Curtiss, R., III 3rd, Secretion of virulence determinants by the general secretory pathway in gram-negative pathogens: an evolving story. *Microbes Infect.* **2000**, *2* (9), 1061–72.
- (33) Sargent, F.; Bogsch, E. G.; Stanley, N. R.; Wexler, M.; Robinson, C.; Berks, B. C.; Palmer, T. Overlapping functions of components of a bacterial Sec-independent protein export pathway. *EMBO J.* **1998**, *17* (13), 3640–50.
- (34) Dilks, K.; Rose, R. W.; Hartmann, E.; Pohlschroder, M. Prokaryotic utilization of the twin-arginine translocation pathway: a genomic survey. *J. Bacteriol.* **2003**, *185* (4), 1478–83.
- (35) Arockiasamy, A.; Aggarwal, A.; Savva, C. G.; Holzenburg, A.; Sacchettini, J. C. Crystal structure of calcium dodecin (Rv0379), from *Mycobacterium tuberculosis* with a unique calcium-binding site. *Protein Sci.* **2011**, *20* (5), 827–33.
- (36) Braibant, M.; Gilot, P.; Content, J. The ATP binding cassette (ABC) transport systems of *Mycobacterium tuberculosis*. *FEMS Microbiol Rev.* **2000**, *24* (4), 449–67.
- (37) Jhingani, G. D.; Kumari, S.; Jamwal, S. V.; Kalam, H.; Arora, D.; Jain, N.; Kumaar, L. K.; Samal, A.; Rao, K. V.; Kumar, D.; Nandicoori, V. K. Comparative Proteomic Analyses of Avirulent, Virulent, and Clinical Strains of *Mycobacterium tuberculosis* Identify Strain-specific Patterns. *J. Biol. Chem.* **2016**, *291* (27), 14257–73.
- (38) Shah, S.; Cannon, J. R.; Fenselau, C.; Briken, V. A Duplicated ESAT-6 Region of ESX-5 Is Involved in Protein Export and Virulence of *Mycobacteria*. *Infect. Immun.* **2015**, *83* (11), 4349–61.
- (39) Mukherjee, P.; Sureka, K.; Datta, P.; Hossain, T.; Barik, S.; Das, K. P.; Kundu, M.; Basu, J. Novel role of Wag31 in protection of mycobacteria under oxidative stress. *Mol. Microbiol.* **2009**, *73* (1), 103–19.
- (40) Kang, C. M.; Nyayapathy, S.; Lee, J. Y.; Suh, J. W.; Husson, R. N. Wag31, a homologue of the cell division protein DivIVA, regulates growth, morphology and polar cell wall synthesis in mycobacteria. *Microbiology* **2008**, *154* (3), 725–35.
- (41) Mi, H.; Huang, X.; Muruganujan, A.; Tang, H.; Mills, C.; Kang, D.; Thomas, P. D. PANTHER version 11: expanded annotation data from Gene Ontology and Reactome pathways, and data analysis tool enhancements. *Nucleic Acids Res.* **2017**, *45* (D1), D183–D189.
- (42) Brennan, M. J.; Delogu, G. The PE multigene family: a 'molecular mantra' for mycobacteria. *Trends Microbiol.* **2002**, *10* (5), 246–9.
- (43) Tiwari, B. M.; Kannan, N.; Vemu, L.; Raghunand, T. R. The *Mycobacterium tuberculosis* PE proteins Rv0285 and Rv1386 modulate innate immunity and mediate bacillary survival in macrophages. *PLoS One* **2012**, *7* (12), e51686.
- (44) Gurvitz, A. The essential mycobacterial genes, fabG1 and fabG4, encode 3-oxoacyl-thioester reductases that are functional in yeast mitochondrial fatty acid synthase type 2. *Mol. Genet. Genomics* **2009**, *282* (4), 407–16.
- (45) Mawunyege, K. G.; Forst, C. V.; Dobos, K. M.; Belisle, J. T.; Chen, J.; Bradbury, E. M.; Bradbury, A. R.; Chen, X. *Mycobacterium tuberculosis* functional network analysis by global subcellular protein profiling. *Mol. Biol. Cell* **2004**, *16* (1), 396–404.
- (46) Marmiesse, M.; Brodin, P.; Buchrieser, C.; Gutierrez, C.; Simoes, N.; Vincent, V.; Glaser, P.; Cole, S. T.; Brosch, R. Macro-array and bioinformatic analyses reveal mycobacterial 'core' genes, variation in the ESAT-6 gene family and new phylogenetic markers for the *Mycobacterium tuberculosis* complex. *Microbiology* **2004**, *150* (2), 483–96.
- (47) Kumar, C. M.; Khare, G.; Srikanth, C. V.; Tyagi, A. K.; Sardesai, A. A.; Mande, S. C. Facilitated oligomerization of mycobacterial GroEL: evidence for phosphorylation-mediated oligomerization. *J. Bacteriol.* **2009**, *191* (21), 6525–38.
- (48) Haslbeck, M.; Franzmann, T.; Weinfurter, D.; Buchner, J. Some like it hot: the structure and function of small heat-shock proteins. *Nat. Struct. Mol. Biol.* **2005**, *12* (10), 842–6.
- (49) Gillis, T. P.; Miller, R. A.; Young, D. B.; Khanolkar, S. R.; Buchanan, T. M. Immunochemical characterization of a protein associated with *Mycobacterium leprae* cell wall. *Infect. Immun.* **1985**, *49* (2), 371–7.
- (50) Canova, M. J.; Kremer, L.; Molle, V. The *Mycobacterium tuberculosis* GroEL1 chaperone is a substrate of Ser/Thr protein kinases. *J. Bacteriol.* **2009**, *191* (8), 2876–83.
- (51) Sassetti, C. M.; Boyd, D. H.; Rubin, E. J. Genes required for mycobacterial growth defined by high density mutagenesis. *Mol. Microbiol.* **2003**, *48* (1), 77–84.
- (52) Dosanjh, N. S.; Rawat, M.; Chung, J. H.; Av-Gay, Y. Thiol specific oxidative stress response in *Mycobacteria*. *FEMS Microbiol. Lett.* **2005**, *249* (1), 87–94.
- (53) Mangan, J. A.; Laing, K. G.; Hinds, J.; Young, D. B.; Butcher, P. D.; Stewart, G. R.; Wernisch, L.; Stabler, R. Dissection of the heat-shock response in *Mycobacterium tuberculosis* using mutants and microarrays. *Microbiology* **2002**, *148* (10), 3129–38.
- (54) Butcher, P. D.; Betts, J.; Banerjee, D. K.; Monahan, I. M. Differential expression of mycobacterial proteins following phagocytosis by macrophages. *Microbiology* **2001**, *147* (2), 459–71.
- (55) Roberts, D. M.; Personne, Y.; Ollinger, J.; Parish, T. Proteases in *Mycobacterium tuberculosis* pathogenesis: potential as drug targets. *Future Microbiol.* **2013**, *8* (5), 621–31.
- (56) Zhao, Q. J.; Xie, J. P. *Mycobacterium tuberculosis* proteases and implications for new antibiotics against tuberculosis. *Crit. Rev. Eukaryotic Gene Expression* **2011**, *21* (4), 347–61.
- (57) Ollinger, J.; O'Malley, T.; Kesicki, E. A.; Odingo, J.; Parish, T. Validation of the essential ClpP protease in *Mycobacterium tuberculosis* as a novel drug target. *J. Bacteriol.* **2012**, *194* (3), 663–8.

- (58) Ribeiro-Guimaraes, M. L.; Pessolani, M. C. Comparative genomics of mycobacterial proteases. *Microb. Pathog.* **2007**, *43* (5–6), 173–8.
- (59) Chaba, R.; Raje, M.; Chakraborti, P. K. Evidence that a eukaryotic-type serine/threonine protein kinase from *Mycobacterium tuberculosis* regulates morphological changes associated with cell division. *Eur. J. Biochem.* **2002**, *269* (4), 1078–85.
- (60) Av-Gay, Y.; Jamil, S.; Drews, S. J. Expression and characterization of the *Mycobacterium tuberculosis* serine/threonine protein kinase PknB. *Infect. Immun.* **1999**, *67* (11), 5676–82.
- (61) Betts, J. C.; Lukey, P. T.; Robb, L. C.; McAdam, R. A.; Duncan, K. Evaluation of a nutrient starvation model of *Mycobacterium tuberculosis* persistence by gene and protein expression profiling. *Mol. Microbiol.* **2002**, *43* (3), 717–31.
- (62) Griffin, J. E.; Gawronski, J. D.; Dejesus, M. A.; Ioerger, T. R.; Akerley, B. J.; Sasseti, C. M. High-resolution phenotypic profiling defines genes essential for mycobacterial growth and cholesterol catabolism. *PLoS Pathog.* **2011**, *7* (9), e1002251.
- (63) Kruh, N. A.; Troudt, J.; Izzo, A.; Prenni, J.; Dobos, K. M. Portrait of a pathogen: the *Mycobacterium tuberculosis* proteome in vivo. *PLoS One* **2010**, *5* (11), e13938.
- (64) Walters, S. B.; Dubnau, E.; Kolesnikova, I.; Laval, F.; Daffe, M.; Smith, I. The *Mycobacterium tuberculosis* PhoPR two-component system regulates genes essential for virulence and complex lipid biosynthesis. *Mol. Microbiol.* **2006**, *60* (2), 312–30.
- (65) Perez, E.; Samper, S.; Bordas, Y.; Guilhot, C.; Gicquel, B.; Martin, C. An essential role for phoP in *Mycobacterium tuberculosis* virulence. *Mol. Microbiol.* **2001**, *41* (1), 179–87.
- (66) de Souza, G. A.; Leversen, N. A.; Malen, H.; Wiker, H. G. Bacterial proteins with cleaved or uncleaved signal peptides of the general secretory pathway. *J. Proteomics* **2011**, *75* (2), 502–10.
- (67) Mattow, J.; Jungblut, P. R.; Schaible, U. E.; Mollenkopf, H. J.; Lamer, S.; Zimny-Arndt, U.; Hagens, K.; Muller, E. C.; Kaufmann, S. H. Identification of proteins from *Mycobacterium tuberculosis* missing in attenuated *Mycobacterium bovis* BCG strains. *Electrophoresis* **2001**, *22* (14), 2936–46.
- (68) Voskuil, M. I.; Schnappinger, D.; Visconti, K. C.; Harrell, M. I.; Dolganov, G. M.; Sherman, D. R.; Schoolnik, G. K. Inhibition of respiration by nitric oxide induces a *Mycobacterium tuberculosis* dormancy program. *J. Exp. Med.* **2003**, *198* (5), 705–13.
- (69) Sherman, D. R.; Voskuil, M.; Schnappinger, D.; Liao, R.; Harrell, M. I.; Schoolnik, G. K. Regulation of the *Mycobacterium tuberculosis* hypoxic response gene encoding alpha-Crystallin. *Proc. Natl. Acad. Sci. U. S. A.* **2001**, *98* (13), 7534–9.
- (70) Baughn, A. D.; Rhee, K. Y. Metabolomics of Central Carbon Metabolism in *Mycobacterium tuberculosis*. *Microbiol. Spectrum* **2014**, *2* (3), 1.
- (71) Barry, C. E. 3rd, Interpreting cell wall 'virulence factors' of *Mycobacterium tuberculosis*. *Trends Microbiol.* **2001**, *9* (5), 237–41.
- (72) Philips, J. A.; Ernst, J. D. Tuberculosis pathogenesis and immunity. *Annu. Rev. Pathol.: Mech. Dis.* **2012**, *7*, 353–84.
- (73) Humpel, A.; Gebhard, S.; Cook, G. M.; Berney, M. The SigF regulon in *Mycobacterium smegmatis* reveals roles in adaptation to stationary phase, heat, and oxidative stress. *J. Bacteriol.* **2010**, *192* (10), 2491–502.
- (74) Yuan, Y.; Crane, D. D.; Barry, C. E. 3rd, Stationary phase-associated protein expression in *Mycobacterium tuberculosis*: function of the mycobacterial alpha-Crystallin homolog. *J. Bacteriol.* **1996**, *178* (15), 4484–92.
- (75) McCune, R. M., Jr.; Tompsett, R. Fate of *Mycobacterium tuberculosis* in mouse tissues as determined by the microbial enumeration technique. I. The persistence of drug-susceptible tubercle bacilli in the tissues despite prolonged antimicrobial therapy. *J. Exp. Med.* **1956**, *104* (5), 737–62.
- (76) Wallace, J. G. The heat resistance of tubercle bacilli in the lungs of infected mice. *Am. Rev. Respir. Dis.* **1961**, *83*, 866–71.
- (77) Kolter, R.; Siegle, D. A.; Tormo, A. The stationary phase of the bacterial life cycle. *Annu. Rev. Microbiol.* **1993**, *47*, 855–74.
- (78) Gee, C. L.; Papavinasundaram, K. G.; Blair, S. R.; Baer, C. E.; Falick, A. M.; King, D. S.; Griffin, J. E.; Venghatakrishnan, H.; Zukauskas, A.; Wei, J. R.; Dhiman, R. K.; Crick, D. C.; Rubin, E. J.; Sasseti, C. M.; Alber, T. A phosphorylated pseudokinase complex controls cell wall synthesis in mycobacteria. *Sci. Signaling* **2012**, *5* (208), ra7.